



Shear Resistance Mechanisms of Steel Sheet Walls with Burrings Holes and the Effect of Wall Widths with Vertical Slits

Yoshimichi Kawai¹, Kazunori Fujihashi², Shigeaki Tohnai³, Atsushi Sato⁴, Tetsuro Ono⁵

Abstract

Shear walls containing 2.73-m-long × 0.455-m-wide steel sheets with vertically aligned burring holes are employed in multi-story buildings in seismically active regions. A configuration with burrs on the inside enables the construction of thinner walls and simplified attachment of finishing. The machining of equipment and piping holes at the construction site can be omitted by the holes. In-line 1.82-, 2.73-, and 3.64-m-wide walls are employed in the buildings, with at least one vertical slit every 0.91-m-wide. The purpose of this study is to clarify the shear resistance mechanisms of walls with burring holes and the effects of wall widths with and without vertical slits. The wall that receives the in-plane shear force allows shear stress to concentrate in the intervals between the holes. Finite element analysis and shear experiments revealed that all intervals between the holes were simultaneously deformed and that the buckling areas in the intervals were restricted by the use of ring-shaped burring ribs of the holes. The post-buckling behavior was dependent on the shapes of the tension field on the intervals. The effect of vertical slits involved maintaining wall strength stable in the inelastic region. The formulas of the allowable design strength and the indexes of strength after shear buckling were developed.

1. Design concept of steel shear walls with burring holes

Shear walls are panels in which steel sheets with burring holes aligned vertically were fastened to studs and tracks. The walls were employed in mid-rise buildings in places requiring seismic resistances. The machining of various holes for equipment and piping can be omitted (Figs. 1, 2).

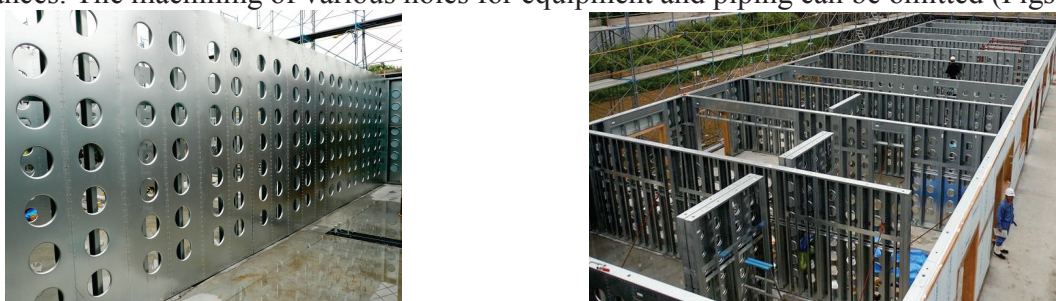


Figure 1: Steel sheet shear walls with burring holes in a 4-story building

¹ Senior Researcher, Nippon Steel & Sumitomo Metal Corp., <kawai.q9z.yoshimichi@jp.nssmc.com>

² Manager, NS Hi-Parts Corp., <fujihashi.ap5.kazunori@jp.nssmc.com>

³ Senior Manager, Nippon Steel & Sumitomo Metal Corp., <tohnai.673.shigeaki@jp.nssmc.com>

⁴ Assoc. Prof., Nagoya Institute of Technology, <sato.atsushi@nitech.ac.jp>

⁵ Professor Emeritus, Nagoya Institute of Technology, <tetsu@sugiyama-u.ac.jp>

Burring holes were created by cold pressing a steel sheet with in-line small-radius holes. A configuration with burrs on the inside and smooth walls on the outside enables the construction of thinner walls and simplified attachments of finishing (Kawai 2016). The mechanisms for standard 2.73-m-high walls with burring holes and the effects of cross-rails were investigated by finite element analysis (FEA) and cyclic loading shear wall experiments (Kawai 2017). The effects of high walls, with the highest size being 4.53 m for the stores and warehouses, were investigated (Kawai 2018). In contrast, steel shapes with burring holes for joists, beams and girders were developed based on the results of previous research (Sato 2014).

This study aimed to clarify the shear resistance mechanisms of wide shear walls with burring holes and the effects of vertical slits. The wide walls were applied to the boundary and north-face walls of the apartment and condominium complexes (Fig. 1). The target 1.82-, 2.73-, and 3.64-m-wide walls are developed for the complexes with at least one vertical slit every 0.91 m. The purpose of the vertical slits is simplified structural calculations to be treated the wide walls as cumulative summed 0.91m unit walls (Fig. 2). The behavior of various wide walls with and without vertical slits was investigated. A comparison of these walls is presented in Section 2.2.

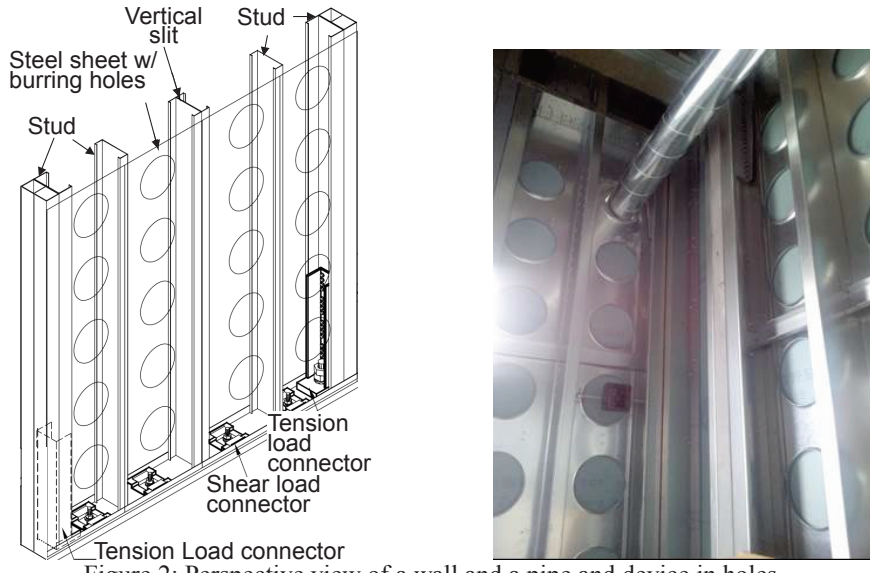


Figure 2: Perspective view of a wall and a pipe and device in holes

2. Resistance mechanisms of wide shear walls with burring holes and vertical slits (FEA)

The shear behavior of the walls was investigated via FEA (MSC. MARC 2014) to estimate the seismic resistance capacities based on the effects of wall widths with vertical slits.

2.1 Specifications of wide shear walls with burring holes

The schematic of 0.91-, 1.82-, and 2.73-m-wide shear walls are shown in Figs. 3~5, respectively. The walls containing 2.73-m-long \times 0.455-m-wide steel sheets with vertically aligned seven burring holes (diameter = 200 mm) with a pitch of 321.6 mm. The steel sheet is hot-dip zinc-aluminum-magnesium alloy-coated steel (JIS SGMC400; nominal yield stress = 295 N/mm²; nominal thickness = 1.2 mm). The four edges of the steel sheet connect to the frame members (studs and tracks) using drilling screw (diameter = 4.8 mm). A burring hole contains rib of curvature radius = 10 mm and cylinder portion (Fig. 3). Both wall end studs are built-up members (BOX-75×75×2.2, two members + C-150×75×15×3.0 + [-142×50×3.0]) and

connected to anchor bolts via tension load connector (Figs. 2, 3). The center stud is one member (C-150×44.5×12×2.2). A stud used for a vertical slit is a built-up member (C-150×75×15×3.0, two members) (Figs. 2, 4) and the center part of 1.638 m is not connected portion (vertical slit). The upper and lower edges of vertical slit are the connected portion to transfer the shear loads.

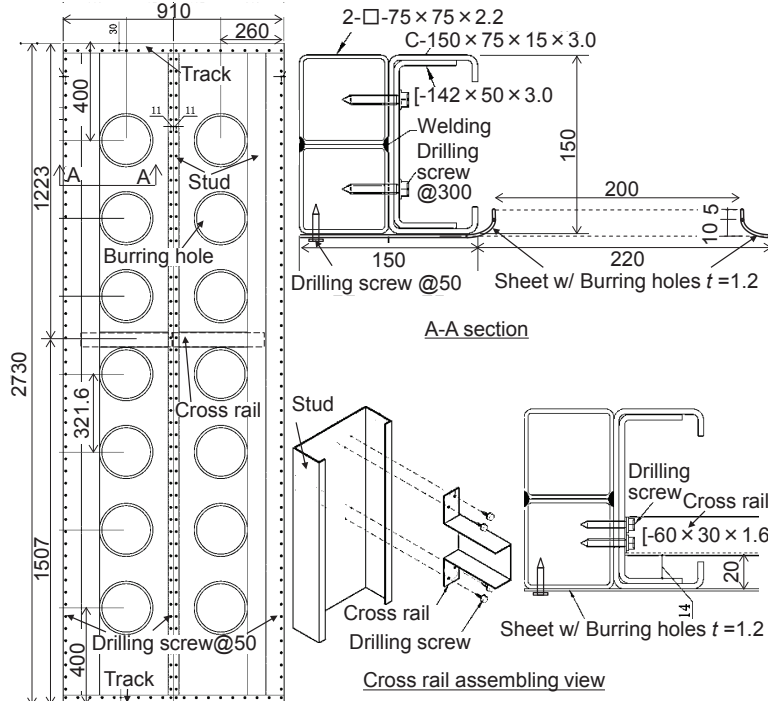


Figure 3: Sectional view of a 0.91-m-wide unit wall (one panel; unit: mm)

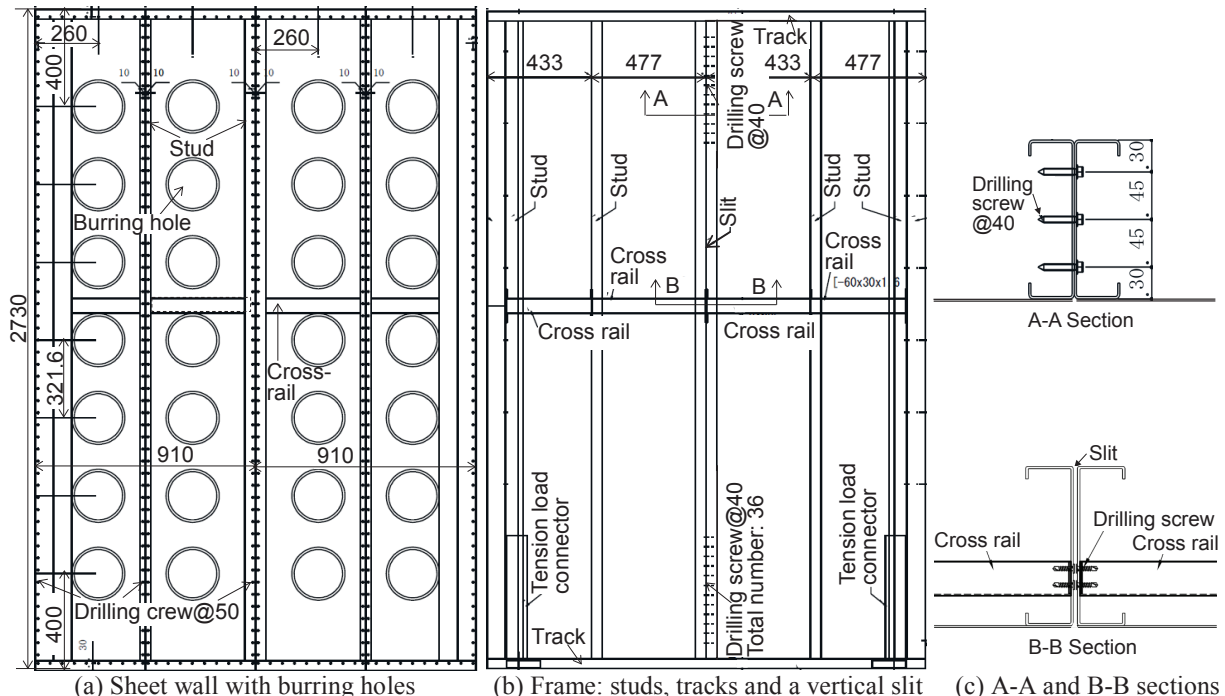
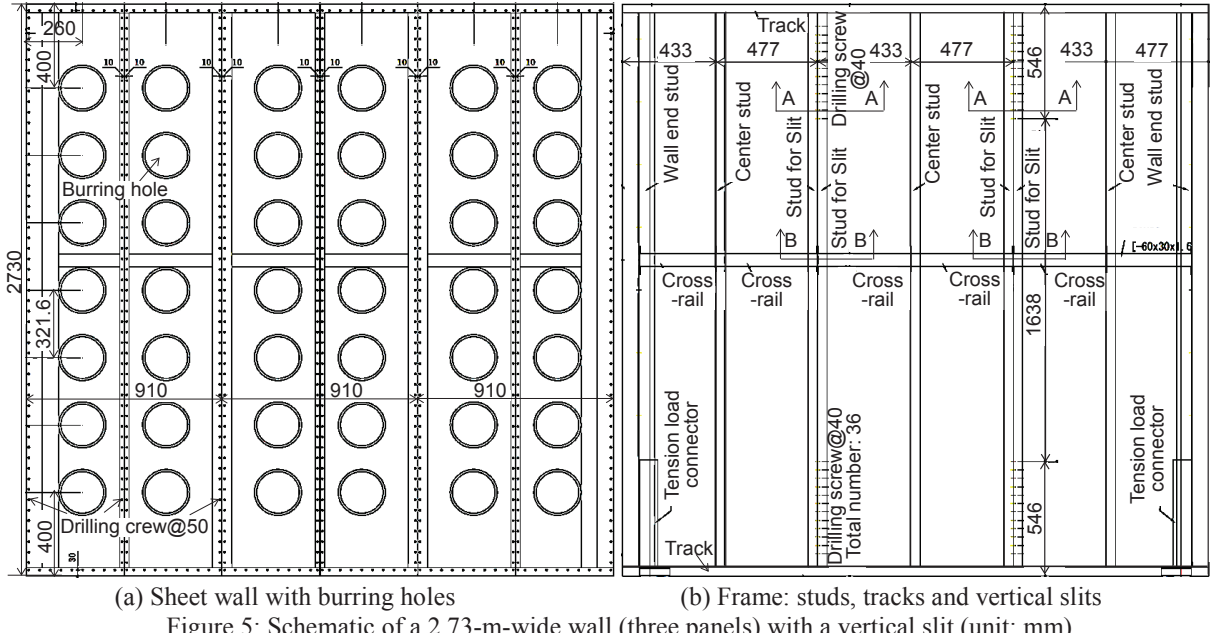


Figure 4: Schematic of a 1.82-m-wide wall (two panels) with a vertical slit (unit: mm)



(a) Sheet wall with burring holes

(b) Frame: studs, tracks and vertical slits

Figure 5: Schematic of a 2.73-m-wide wall (three panels) with a vertical slit (unit: mm)

The steel sheets with burring holes were modeled using shell elements (Fig. 6a) and the mechanical properties were modeled as poly-linear stress-strain curves (Fig. 6b). The drilling screw connections were modeled using shear springs based on the experimental results of previous research (Fig. 6c) (Azuma 2006, Toriyama 2013). The studs, tacks and cross-rails were modeled by elastic members. The cross-rails had 1/1000 deflection spline curves representing the eccentricity of the end joints. One-way forced displacement was placed on the top of the wall, and pin support connections were placed at the bottom of the wall, like the cantilever structure.

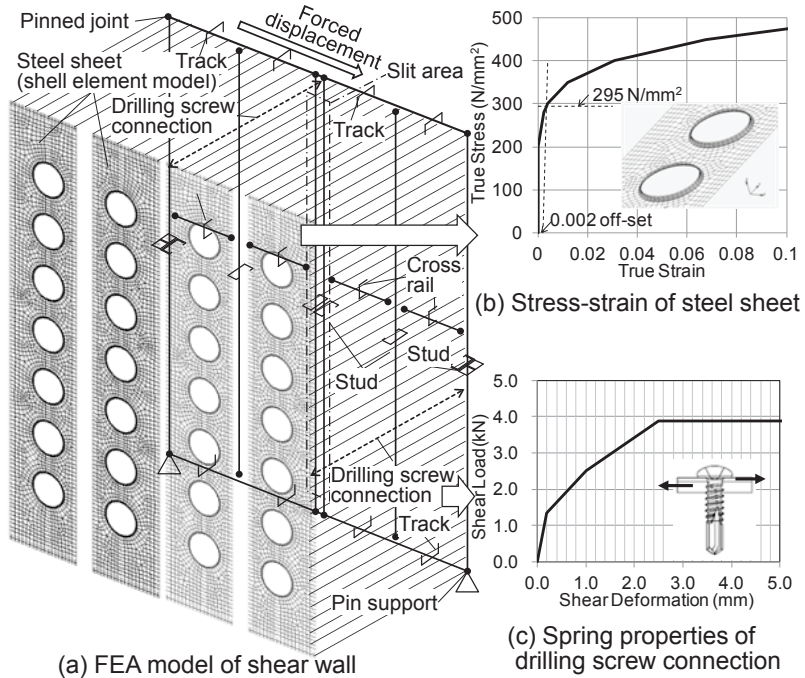


Figure 6: Finite element analysis (FEA) model of shear wall (two panels)

2.2 Behavior of wide walls with burring holes and vertical slits (FEA)

The relation between shear load per 0.91-m-wide panel and story angle of the walls shows linear stiffness in the elastic region until 1/300 wall story angle (Fig. 7). The walls drastically change from the elastic to plastic regions and maintain stable strength until the ultimate state. The variable-width walls with vertical slits show almost same behavior and lower strength than the 0.91-m-wide wall (one panel) at 1/100 story angle. The larger the number of vertical slits in a wide wall, the slightly lower the shear load is at around 1/100 story angle and above. The walls without vertical slits show continuously increasing shear load and drastically higher than the 1 panel at 1/100 story angle (Table 1). Therefore, vertical slits are necessary for wide walls, using the simplified structural calculations to be treated the walls as cumulative summed 0.91 m ones.

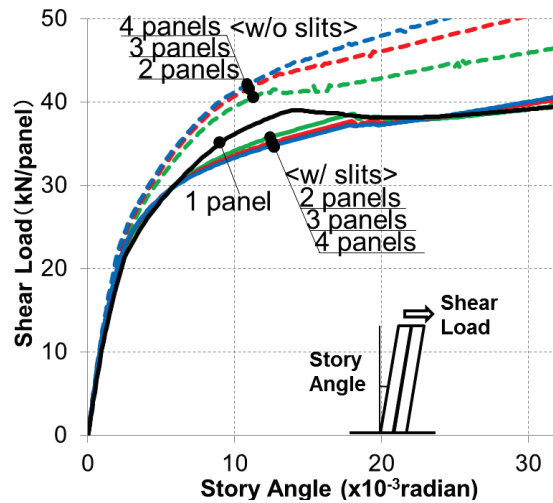


Figure 7: Shear load-story angle relations of shear walls with and without slits

Table 1: Shear load per one panel at story angle of 1/300, 1/200 and 1/100 by FEA

Shear wall	Width [m]	Shear load [kN/panel] at story angle:		
		1/300	1/200	1/100
One panel	0.91	24.2	28.6	36.6
With slits	Two panels	24.9	28.5	34.1
	Three panels	25.2	28.6	33.6
	Four panels	25.3	28.6	33.3
Without slits	Two panels	26.3	31.0	39.4
	Three panels	27.0	31.9	40.7
	Four panels	27.3	32.3	41.2

The contour of the von Mises stresses and 1/1 deformation at the bottom left parts of the walls, taken from the inclined bottom views, exhibit stress concentrations at the intervals between the holes at 1/300 story angle, and they experience simultaneous anti-plane deformation at all intervals at 1/100 story angle (Fig. 8). The deformations are limited in the intervals, and a large out-of-plane waveform in a sheet is effectively prevented by the ring-shaped ribs of the holes. The 3.64-m-wide walls (four panels) with and without vertical slits are compared, and the stress directions in the principal stress flow are indicated by arrows (Figs. 8b,c). The wall without vertical slits at 1/300 and 1/100 story angles have ordered stress flow along the tangent lines that diagonally connect the ribs of the lined holes, while the wall with vertical slits at 1/100 story angle has disordered stress flows. The 0.91-m-wide unit walls (one panel) at 1/300 and 1/100 story angles have ordered stress flow (Fig. 8a) same as the wall without vertical slits (Fig. 8c).

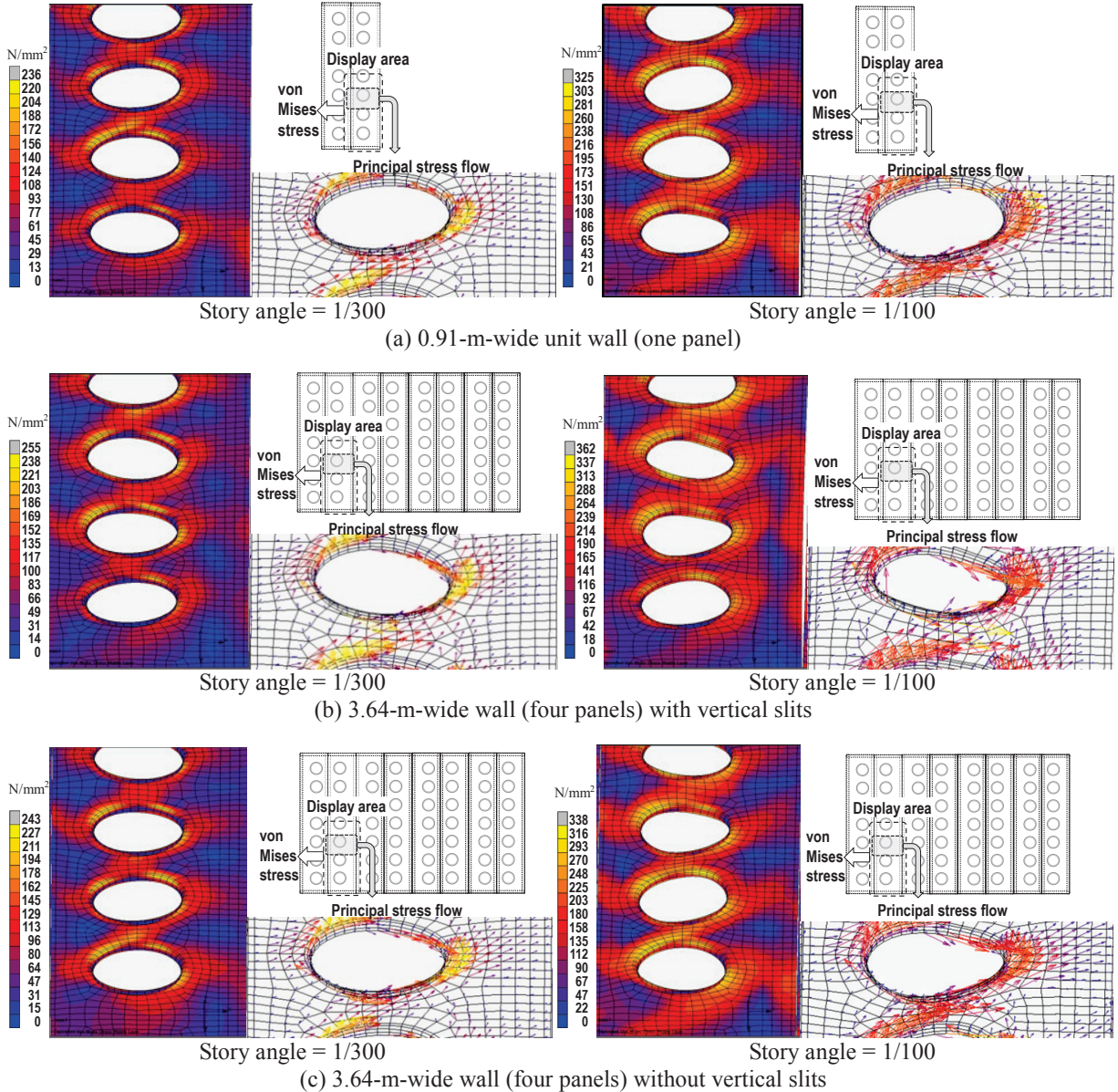


Figure 8: von-Mises stress (left-hand side) and principal stress (right-hand side) and deformation ($\times 1.0$)

The shear stresses at the center of the intervals on the vertical section between the holes are shown in Fig. 9. The 3.64-m-wide walls (four panels) with and without vertical slits are compared. The shear stresses of the walls without vertical slits are almost the same from the initial to ultimate state regions (Fig. 9b), while those of the walls with vertical slits are disordered after the elastic limit (Fig. 9a). These differences cause shear load differences between the walls with and without vertical slits in Fig. 7. The horizontal shear forces at each drilling screw connection between the sheets and studs at the same height of the far left side of the wide walls are shown in Fig. 10. The wide walls with vertical slits exhibit smaller horizontal shear forces at all connections than the forces of one panel (Fig. 10a). The larger the number of vertical slits in a wide wall, the slightly lower the forces at the connections. The wide walls without vertical slits exhibit larger horizontal shear forces at all connections than the forces of one panel (Fig. 10b). The walls without vertical slits develop tension fields that prevent the deformation of burring

holes and order the stress flows at the intervals shown Fig. 8c owing to the use of shear forces at drilling screw connections. The mean values of the shear forces at drilling screw connections on the left and right steel sheets of far left side unit of walls are listed in Table 2. The mean values are normalized by the values of 0.91-m-wide wall (one panel). The normalized values α_λ are used for developing the formula for strength indexes after shear buckling in Section 3.

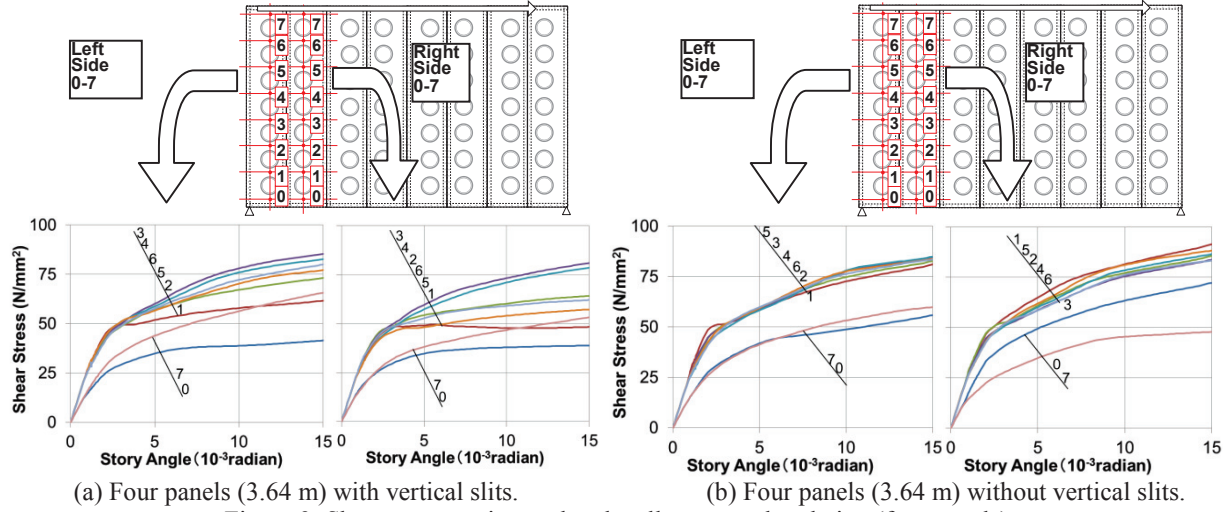


Figure 9: Shear stress on interval and wall story angle relation (four panels)

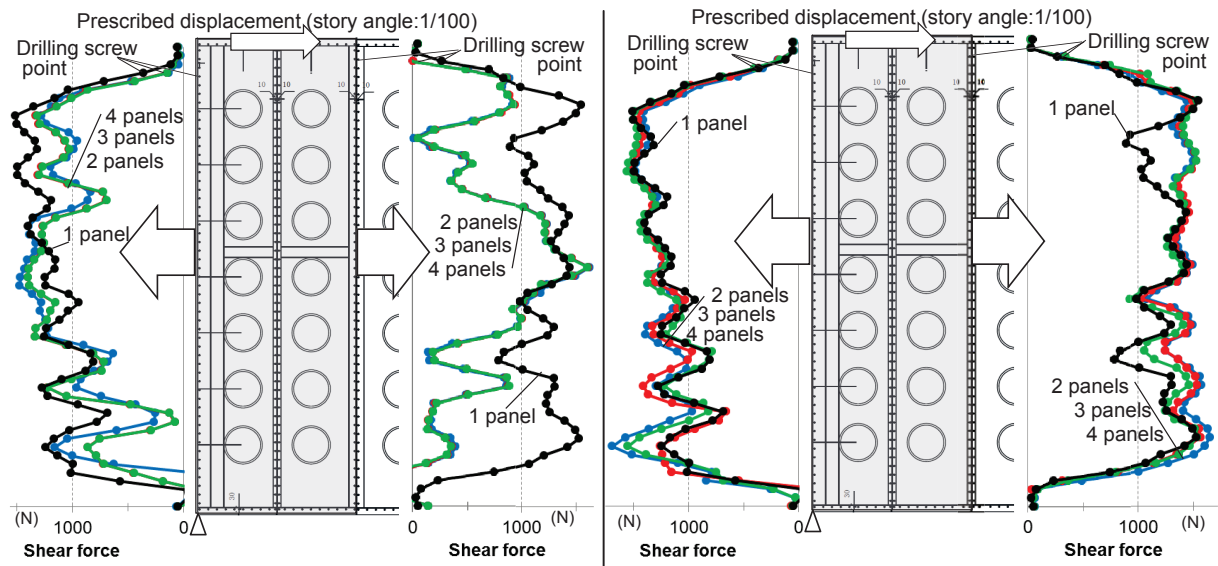


Figure 10: Horizontal shear forces at screw connections on a steel sheet and a stud (wall story angle = 1/100)

Table 2: The mean values of the shear forces at drilling screw connections on a steel sheet and studs

Shear wall at 1/100 story angle	Width [m]	Mean value of shear forces [N/screw]		α_λ = ratio normalized by the value of one panel	
		Left side	Right side	Left side (α_1)	Right side (α_2)
One panel	0.91	1058	1093	1.00	1.00
With slits	Two panels	882	594	0.83	0.54
	Three panels	887	598	0.84	0.55
	Four panels	888	594	0.84	0.54
With- out slits	Two panels	1117	1203	1.06	1.10
	Three panels	1114	1240	1.05	1.13
	Four panels	1142	1258	1.08	1.15

3. Design strength formula for wide steel shear walls with burring holes and vertical slits

The formulas of allowable design strength and the indexes of strength after buckling of the wide steel shear walls and burring holes and vertical slits are developed for the serviceability limit state and the ultimate limit state of the buildings, respectively.

3.1 Allowable design strength formula

Based on the mechanism of shear resistance of the walls with burring holes and vertical slits, the allowable design strength is derived. The wall drastically changes from the elastic region to plastic region because of shear buckling, which simultaneously occurs at all intervals between the holes (Figs. 7, 8). The stress in an interval is no uniform, but the likeliness of the occurrence of buckling depends on the flat rectangular plate area that includes the interval, whose diagonal constitutes the tangent line on which the buckling waveforms are located (Fig. 11a). The other areas between the holes and the upper or lower edges of a sheet are extracted (Figs. 11b, c). The allowable strength design value of a wall per 0.91-m-wide panel is obtained by summing the buckling strength of the intervals in the vertical direction (Eqs. 1~4).

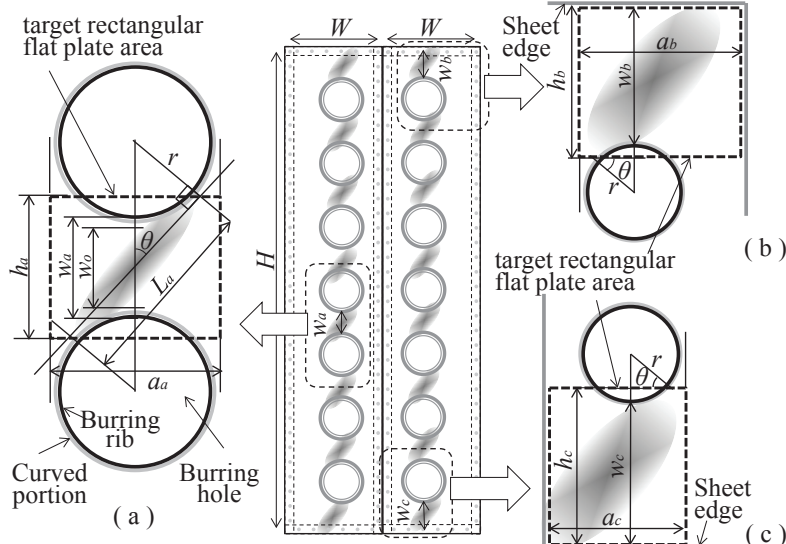


Figure 11: Target rectangular flat-plate areas for the shear buckling design

$$Q_a = 2 \cdot [\tau_a \cdot w_a \cdot t(n-1) + \tau_b \cdot w_b \cdot t + \tau_c \cdot w_c \cdot t] \cdot (W/H) \quad (1)$$

$$\tau_i = k_{vi} \cdot \pi^2 \cdot E \cdot \left\{ (t/h_i)^2 / [12 \cdot (1 - \nu^2)] \right\} \quad i = a, b, c \quad (2)$$

$$(a_i/h_i) \leq 1.0 \quad k_{vi} = 4.0 + 5.34 \cdot (h_i/a_i)^2, \quad (a_i/h_i) > 1.0 \quad k_{vi} = 5.34 + 4.0 \cdot (h_i/a_i)^2 \quad (3)$$

$$wQ_a = m \cdot Q_a \quad (4)$$

Here, Q_a is the allowable shear strength per 0.91-m-wide panel (one panel). τ_a , τ_b , and τ_c are shear buckling stresses at the intervals derived from Eq. 2 (AISI 2007). w_a , w_b , and w_c are the widths of the intervals. t is the thickness, and n is the number of burring holes. W and H are the wall width and height. E is the modulus of elasticity, ν is Poisson's ratio. r is the radius of the burring holes, L_a is $2\sqrt{(r+w_0/2)^2 - r^2}$, h_a is $L_a \cos \theta$ and a_a is $2r$. wQ_a is the allowable shear strength of wide walls and m is the number of panels. The design values using Eq. 1 are shown in Table 4.

3.2 Strength index at 1/100 story angle

The walls with burring holes and vertical slits maintain stable strength (Fig. 7). The strength at 1/100 story angle is used as the index to evaluate the ultimate strength. The wall width has a little effect on the strength, and vertical slits decrease the shear strength. The larger the number of vertical slits in a wall, the slightly lower the shear load is at around 1/100 story angle and above. Therefore, the basic mechanism of the wall with vertical slits is developed (Fig. 12). The tension in an interval between the holes balances with a compression of $Q_a/2$ resisted by a burring hole. Q_a is equal to the allowable strength for the wall per 0.91-m-wide panels. The horizontal shear forces at screw connections per burring hole, $2k \cdot \alpha_\lambda \cdot \delta_1/2$, are added to $Q_a/2$, which balances with the shear strength of the 0.455-m-wide half size panel at 1/100 story angle, $\lambda Q_u/2$, in Eq. 5. The coefficient α_λ ($\lambda=1,2$) is the normalized value derived from Table 2, and 0.84 for the 1/2 panel between the wall end stud and the center stud ($\lambda=1$), 0.54 for the 1/2 panel between the slit stud and the center stud ($\lambda=2$). The wide wall strength at 1/100 story angle per 0.91-m-wide panel Q_u is derived as follows.

$$\lambda Q_u / 2 = Q_a / 2 + (2 \cdot k \cdot \alpha_\lambda) \cdot (\delta_1 / 2) \quad (\lambda = 1,2) \quad (5)$$

$$\delta_2 = \frac{(\lambda Q_u / 2) / \sin \theta}{E \cdot (w_0 / 2) \cdot \sin \theta \cdot t} \cdot L / \sin \theta = \frac{(\lambda Q_u / 2) \cdot L}{E \cdot (w_0 / 2) \cdot \sin^3 \theta \cdot t} \quad (6)$$

$$\frac{\delta}{\beta \cdot r} = \frac{\delta_1 + \delta_2}{\beta \cdot r} = \frac{(\lambda Q_u / 2 - Q_a / 2) / (k \cdot \alpha_\lambda) + \lambda Q_u \cdot L / (E \cdot w_0 \cdot t \cdot \sin^3 \theta)}{\beta \cdot r} = 1/100. \quad (7)$$

$$\lambda Q_u / 2 = \left[\frac{\beta \cdot r / 100 + Q_0 / (2k \cdot \alpha_\lambda)}{1 / (k \cdot \alpha_\lambda) + L / (E \cdot w_0 / 2 \cdot t \cdot \sin^3 \theta)} \right] \quad (8)$$

$$Q_u = (Q_u + Q_u \cdot (m-1)) / m \quad (m \geq 2) \quad (9)$$

Here, w_o is the width of the interval between holes without burring ribs, β is the ratio of pitch to the radius of the holes, $w_o/2$ is the width of the tension field at the interval, and m is the number of panels. $2k \cdot \alpha \cdot \delta_1/2$ is derived from cross-rails that charge the compressions between middle points of side-by-side-laying cross-rails or tracks. The cross-rail charges 3.5 holes and $2k$ is 10.0 kN/mm (Kawai 2017). Table 5 provides of a comparison of the strength values and experimental results.

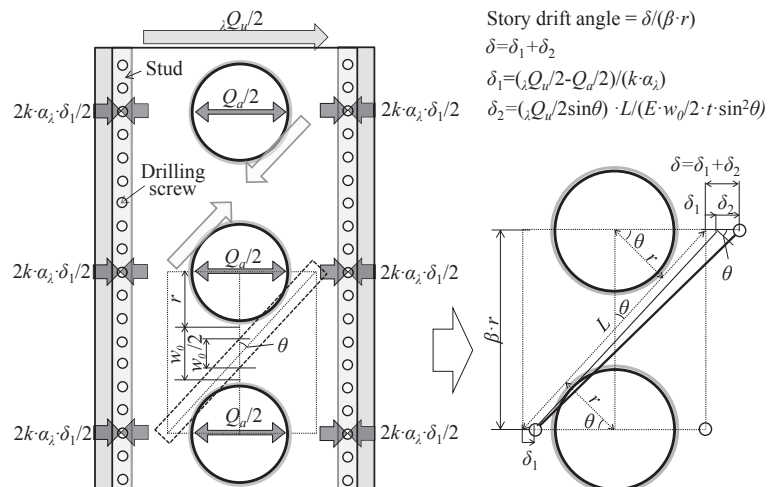


Figure 12: Stress and deformation model at 1/100 angle (1/2 Panel)

4. In-plane cyclic shear test of wide steel shear walls with burring holes and vertical slits

Shearing tests were conducted for wide walls with burring holes and vertical slits to confirm their seismic resistance, failure mechanism, and the applicability of design formulas. The loads were placed on top of the walls (Fig. 13). Three cycles were conducted at the story angles 1/450~1/30 of the wall [Kawai 1999]. The story angles excluded the rotations by the lift of the walls. The specimens were the same as those shown in Figs. 2~5. The mechanical properties and the specifications of the steel sheets, the members and connections are summarized in Table 3.

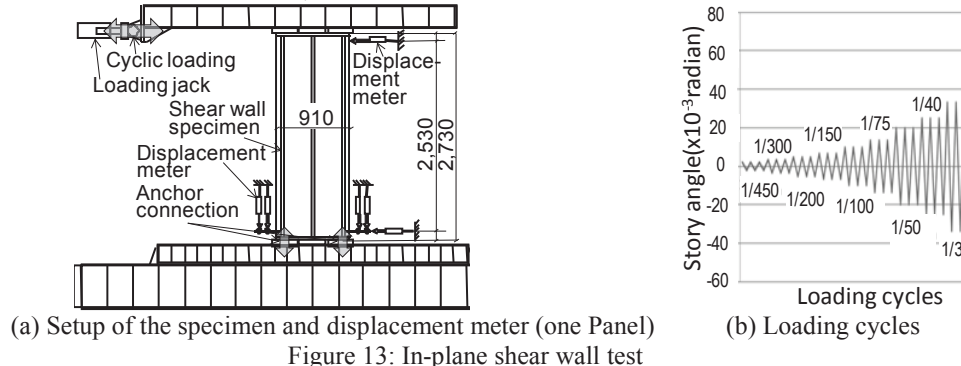


Figure 13: In-plane shear wall test

(a) Setup of the specimen and displacement meter (one Panel)

(b) Loading cycles

Figure 13: In-plane shear wall test

Table 3: Mechanical properties of steel sheets and specifications of members and connections

Member	Standard	Size and mechanical properties
Steel sheet with burring holes		Thickness: 1.23 mm (with coating) and 1.195 mm (without coating) Yield stress: 305 N/mm ² , Tensile strength: 400 N/mm ² , Elongation: 38%
Studs	JIS G3323 SGMC400	Both ends: BOX-75×75×2.2, two members + C-150×75×15×3.0 + [-142×50×3.0] Center: C-150×44.5×12×2.2 Slit: C-150×44.5×12×2.2, two members
Tracks		[−155×40×2.2]
Cross-rails		[−60×30×1.6]
Drilling screw	JIS B1055	Diameter: 4.8 mm; Length: 19 mm
Anchor bolt	JIS B1180	Diameter: 36 mm; Nominal strength: 880 N/mm ²

Fig. 14 shows the behavior of the 0.91-m-wide wall (one panel) at story angle of 1/100 and the bottom left parts of the wall from the view direction of inclined bottom. The wall showed no local deformations at story angle of 1/300 and 1/200 and slight out-of-plane deformations at the all intervals between the holes at story angle of 1/100. The shear buckling waveforms were created, and the deformation areas were limited in the intervals owing to the ring-shaped ribs of the holes at story angle of 1/50. The figures in Fig. 14 are considerably similar to those in Fig. 8 obtained by FEA. The photos of 1.82-(two panels), 2.73-(three panels) and 3.64-m-(four panels)-wide walls used in the experiment indicate out-of-plane deformations at the all intervals between the holes at story angles of 1/100 (Figs. 15 a~c, respectively). The shear buckling waveforms were created on the tangents that diagonally connect the vertical holes. The deformation areas were limited in the intervals owing to the ring-shaped ribs of the holes. The relations between in-plane shear load and story angle of the wall specimens are shown in Figs. 16a~d. All walls showed significant stiffness in the initial, and the stiffness drastically changed from the elastic region to plastic region. The walls maintained high strength until the ultimate state was reached, but the shear loads were proportional to the wall width. The effects of the vertical slits on wide walls were to be treated the walls as cumulative summed 0.91-m ones. Under cyclic loading, the shear load-story angle relations exhibited pinching behavior with stable round loops, which efficiently absorb the seismic energy. The shear load in the second cycle at the same story angle decreased slightly, while the shear load in the third cycle did not decrease further.

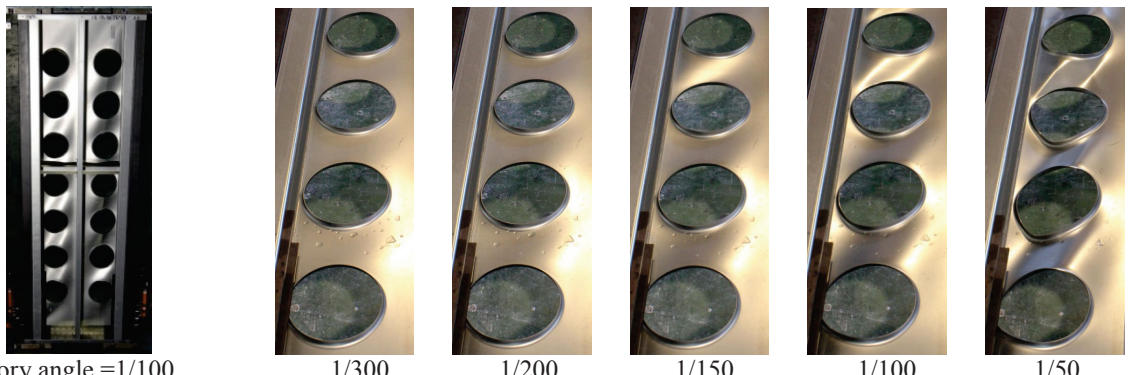


Figure 14: Behavior at maximum story angles of each loading cycle at 0.91-m-wide wall (one panel)

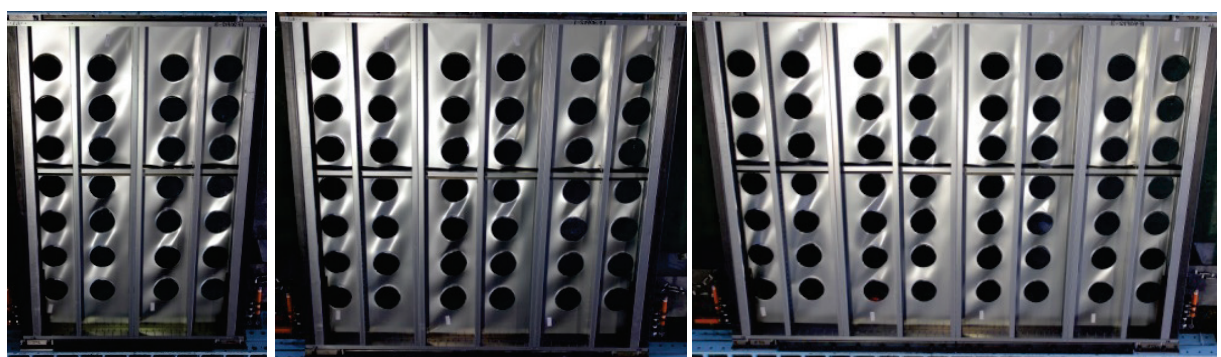


Figure 15: Behavior of shear walls with burring holes at wall story angle of 1/100

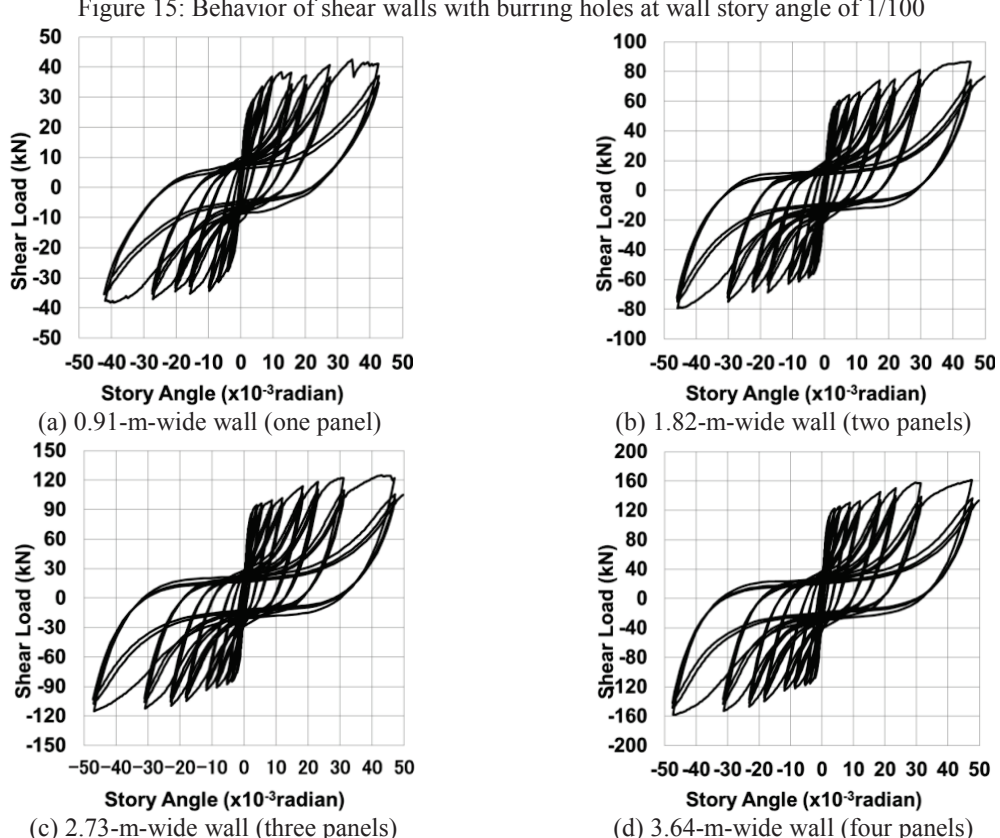


Figure 16: In-plane shear load-story angle relations

The shear load (per 0.91-m-wide pane)–story angle relations of the walls are compared using envelope curves (Fig. 17). The variable-width walls with vertical slits show almost same behavior and lower strength than the 0.91-m-wide wall (one panel) at 1/100 story angle. The larger the number of vertical slits in a wide wall, the slightly lower the shear load is at around 1/100 story angle and above. The allowable shear strengths of the walls derived from Eq. 1 are lower than the strength of the walls at story angles of 1/300 (Table 4). The index strengths of the wall derived from Eq. 9 are almost same as shear loads at 1/100 story angle obtained via experiments (Table 5).

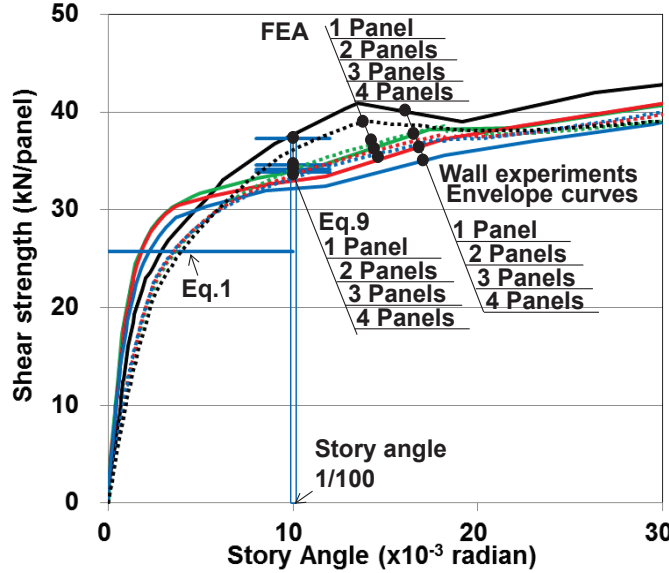


Figure 17: In-plane shear load-story angle relation (envelope curve)

Table 4: Design strength (Eq. 1) and shear load at story angle of 1/300 obtained from experiments and FEA

Shear wall	Width[m]	Experiment[kN/panel]		FEA[kN/panel]	Eq.1 [kN/panel]
One panel	0.91	27.1	26.3	26.6	24.2
Two panels	1.82	30.1	28.6	28.6	24.9
Three panels	2.73	29.9	30.7	29.4	25.2
Four panels	3.64	29.8	30.0	28.6	25.3

Table 5: Index strength (Eq. 9) and shear load at story angle of 1/100 obtained from experiments and FEA

Shear wall	Width[m]	Experiment[kN/panel]		FEA[kN/panel]	Eq.9 [kN/panel]
One panel	0.91	37.7	35.7	35.2	36.6
Two panels	1.82	34.2	32.8	32.5	34.1
Three panels	2.73	33.0	33.5	32.5	33.6
Four panels	3.64	32.2	32.8	32.2	33.3

5. Conclusions

The seismic performances of in-line 1.82-, 2.73- and 3.64-m-wide walls with at least one vertical slit every 0.91m, were investigated via FEA and experiments. The conclusions of this research are summarized as follows:

- The walls exhibited significant stiffness in the initial elastic region, whereas they maintained stable strength under large story angles with simultaneous deformation at all intervals between the holes. Furthermore, the walls showed stable seismic energy absorption capability, as demonstrated by the round loops of the load-story angle curves.
- The walls that experienced in-plane shear forces allowed shear stress to concentrate between the aligned burring holes. Stress concentration finally led to the ultimate state because of

- shear buckling, and the buckling areas in the intervals were restricted by the use of ring-shaped ribs of the holes.
- The initial elastic strengths until the serviceability limit of a story angle of 1/300 for all walls were almost the same, regardless of the wall width.
 - The post-buckling behavior depended on the shapes of the tension field on the intervals. The effect of vertical slits maintained stable wall strength stable in inelastic region.
 - The purpose of the vertical slits, which is simplified structural calculations to be treated the wide walls as cumulative summed 0.91-m-wide unit walls, was confirmed via FEA and shear wall experiments.
 - Based on our analytical and experimental findings, the allowable strength design formula of a wall was developed. The design value was obtained by summing the shear buckling strength of the intervals between the holes in the vertical direction of the wall. The allowable strength design values obtained using the formula lie the lower values at wall story angle of 1/300 obtained through experiments.
 - The index strength at story angle of 1/100 was determined. The tension in an interval was balanced with the compression resisted by burring holes and horizontal shear forces at screw connections. The index values at story angle of 1/100 for the walls were almost same as the shear load values obtained via experiments.
 - The R-value for the evaluation of the seismic performance of shear walls will be discussed in a subsequent report.

Acknowledgments

The authors appreciate the significant contributions made by Makoto Kondo, NS Hi-parts, Tokyo and Yusuke Shimoda, Daiken Information System, Tokyo, in the wall experiments and the FEA.

References

- Y. Kawai, M. Kondo, A. Sato, T. ONO, S. Tohnai. (2016). "Allowable Design Formula for Steel Sheet Shear Walls with Burring Holes." *7th International Conference on CIMS*. Baltimore.
- Y. Kawai, K. Fujihashi, S. Tohnai, A. Sato, T. ONO. (2017). "Shear Resistance Mechanisms on Steel Sheet Shear Walls with Burring Holes and the Effect of Cross-Rails." *9th International Conference on the Behaviour of Steel Structures in Seismic Areas*. Christchurch, New Zealand.
- Y. Kawai, K. Fujihashi, S. Tohnai, A. Sato, T. ONO. (2018). "Shear Resistance Mechanisms on High-Panelized Steel Sheet Walls with Burring Holes." *IABSE Conference*, Kuala Lumpur, Malaysia
- A. Sato, S. Mori, T. Ono, et al. (2014). "Study on Buckling Strength of Light-gage Steel Members with Large Opening." *Proceedings of constructional steel*. Vol.22 716-723.
- K. Azuma, N. Takagi, H. Senda, C. Watanabe, T. Karatsu. (2006). "Application of Fastening System by Self-drilling Tapping Screws." *Proceedings of constructional steel*, Vol.14 705-712.
- T. Toriyama, A. Sato, T. Ono, H. Okada. (2013) "Screw strength of shear lap joint by drill screw connections." *Architectural Institute of Japan*, Tokai.; Vol.51 217-220.
- American Iron and Steel Institute. (2007) AISI Standard North American Specification for the Design of Cold-formed Steel Structural Members.
- K. Sakuragi, A. Sato, T. Ono, S. Hashimoto. (2016). "Ductility Reduction Factor of Steel Sheet Shear Wall with Burring Holes Used in Steel Framed House." *7th International Conference on CIMS*. Baltimore.
- The Japan Iron and Steel Federation. (2002). "Guide for Designing Cold-formed Steel Structures." Gihodosuppan,
- Y. Kawai, R. Kanno, et al. (1999). "Seismic Resistance and Design of Steel-Famed Houses." *Nippon Steel Technical Report*. No.79, 7-16.
- A. Formisano, L. Lombardi. (2016). "Numerical prediction of the non-linear behavior of perforated metal shear panels." *Cogent Engineering*. Vol.3 Issue 1 art. No. 1156279
- A. Formisano, L. Lombardi, F.M. Mazzolani. (2016). "Perforated metal shear panels as bracing devices of seismic-resistant structures." *Journal of Constructional Steel Research*. 126 pp.37-49